Hindawi Publishing Corporation
International Journal of Geophysics
Volume 2014, Article ID 174589, 12 pages
http://dx.doi.org/10.1155/2014/174589

Research Article

Integrated Approach to Investigate the Effect of Leachate on Groundwater around the Ikot Ekpene Dumpsite in Akwa Ibom State, Southeastern Nigeria

N. J. George,[1] A. I. Ubom,[2] and J. I. Ibanga[1]

[1] *Department of Physics, Akwa Ibom State University, Ikot Akpaden, Nigeria*
[2] *Department of Physics, University of Calabar, Cross River State, Nigeria*

Correspondence should be addressed to N. J. George; nyaknojimmyg@gmail.com

Received 8 June 2013; Revised 9 October 2013; Accepted 10 November 2013; Published 28 January 2014

Academic Editor: Michael S. Zhdanov

Geophysical, geochemical, and hydrogeological measurements have been integrated to assess the effect of leachate on groundwater quality within the dumpsite in Ikot Epene Local Government Area of Akwa Ibom State, Southern Nigeria, and its environs. The resistivity values and depth of burial of the geomaterials, constrained by geology, were used in producing resistivity cross sections which show the geoelectric distribution of the subsurface near and away from the dumpsite. The observed high conductivity in subsurface layers closed to the dumpsite is symptomatic of the leachate-loaded conductive fluid leached and drained into the subsurface. The hydrochemical results of some species conform to WHO standards, while some were found to be relatively higher due to dissolution, leaching, and draining of leachate related contaminants in the soil. The correlation indices of the ion pairs show no significant effect on the paired ions, indicating that the significant value of some of the individual ions is not geologic but due to precipitation from the leachate residue. In general, the effect of leachate is more dominant in the immediate groundwater pathway near the dumpsite than aquifer repositories away from it. The crossplots of the water resistivity and bulk resistivity show exponential increase for the different layers.

1. Introduction

Environmental contamination is one of the main concerns of earth scientists and researchers worldwide. The accelerated pace of industrial development coupled with uncontrolled growth of the urban population has resulted in the increasing production of solid/liquid residues. Urban waste materials, mainly domestic garbage, are usually disposed without the appropriate measures of the effect of the released fluid (leachate) on groundwater resources. Groundwater pollution happens mostly due to percolation of pluvial water and the infiltration of contaminants through the soil. The contaminant fluid emanated from the decomposition of organic matter is rich in dissolved salts, containing substantial amount of polluting substances [1, 2]. When the contaminant liquid (leachate) diffuses into the groundwater table, it affects the potability of groundwater, putting the local community into serious health risk. Some of the most frequent demands of people in the metropolitan areas include the detection of the location and extent of contamination patches/plumes in areas such as dumpsites or landfill sites.

Electrical resistivity of soils is dependent up various factors, including soil type, water content, saturation, and pore fluid property. This experimental work has been performed to investigate the relationship between electrical resistivity and surficial subsurface conditions with varying physical property and landfill leachate contamination. The moisture density can be the most effective indicator for describing the relationship between electrical resistivity and physical property of unsaturated subsurface. Experiments by other authors show that the electrical resistivity of soil exponentially decreased as moisture density increased. The addition of leachate fraught with various ions decreases the electrical resistivity. Also, the formation factor can be described by the term of moisture density in unsaturated sand. The formation factor (ratio of bulk resistivity to water

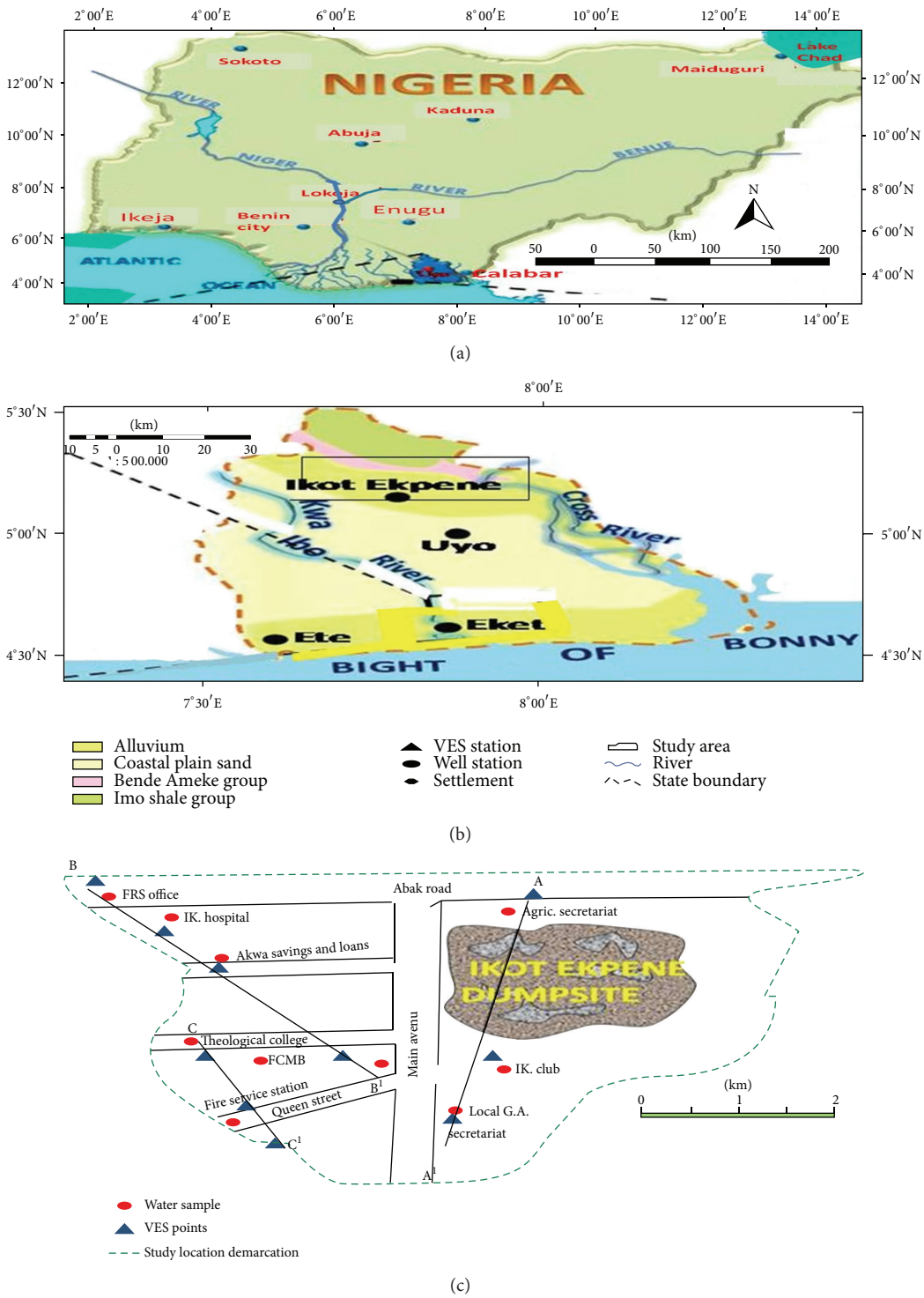

(a)

(b)

(c)

Figure 1: Outline map of (a) Nigeria showing the position of Akwa Ibom State, (b) map of the study area showing some of the LGAs and the generalized geology, and (c) sketch map of the dumpsite location and its environ, showing the VES profiles, boreholes, and VES location.

resistivity of a medium) is higher when soil and pore water are contaminated by higher concentration of leachate than when soil and pore water are uncontaminated, since the movement ions are restrained by electrochemical interactions between soil particles and leachate constituents.

The study area is situated in the northwestern part of Akwa Ibom State in southern Nigeria (Figure 1). In the study area, the primary source of potable water which is utilized for domestic, agricultural, and industrial purposes is groundwater. Shallow aquifers are overexploited through open wells

and bore wells. There has been significant deterioration in groundwater quality due to the leachate emanated from dumpsite into the wells located within the radius of the study area. The impact of leachate in groundwater is stupendous. Although the tissue fluid (leachate) loaded with mobile ions is rich in mineral nutrients needed by plants for agricultural productivity, the main preoccupation of the dwellers in the area, this degraded groundwater is unsuitable for drinking.

To assess the effect of leachate on the quality of groundwater, geophysical, hydrogeological, and hydrochemical studies were carried out near and away from the dumpsite located in the study area. The dumpsite is composed of materials of mechanical, biological, and chemical sources. Since the leachate contaminant is associated with high salinity flows within the subsurface, electrical resistivity method can be the most suitable field method to determine the region of dominant influence of salinity through measurement of apparent electrical resistivity of the subsurface. Under many subsurface conditions, electrical resistivity method can quickly and economically delineate the general level of contaminant/plume and identify areas most feasible for sampling and monitoring. Many contaminants contain ionic concentrations considerably higher than the background level of native groundwater [3]. When such contaminants are introduced into an aquifer, the electrical resistivity of the saturated zone is reduced [4]. Electrical resistivity study across suspected areas of high conductivity or low resistivity can identify such areas as zones fraught with contaminations [5]. However, combining the results from geophysical, hydrogeological, and hydrochemical data of monitoring wells can improve the uniqueness of the results.

Empirical relations between the site dependent earth resistivity (ER) and the measured electrical conductivity (EC) of groundwater can be used to predict the magnitude of contaminant within and away from the dumpsite [5]. The objective of this paper is to integrate geoelectric and physicochemical data in determining the effect of leachate on groundwater within the dumpsite location and its environs. It also attempts to show the relationship between bulk and water resistivity thereby predicting the level of diffusion of dissolved fluid from dumping refuse into the groundwater repositories within the dumpsite environment.

2. Location

The dumpsite and its environs located in Ikot Ekpene Local Government Area (Figure 1) lie between latitudes 5.072°–5.140°N and longitudes 7.390°–7.458°E in Akwa Ibom state, southeastern Nigeria. It spreads over an area of about 25 km^2. The basin is characterized by gently undulating topography with hills located in the northern parts and is sloping towards southwest. The maximum elevation in the area is of the order of 40 m (amsl) in the north whereas the minimum elevation is of the order of 10 m (amsl) in the south. The region is highly drained by the inland coastal water. Vegetation in the study area is of the rain forest type. It is sustained by the tropical climate characterized by high temperature with annual mean of 5.5°-6.5°C. The maximum daily temperature lies between 28° and 30°C during March and the minimum daily mean temperature lies between 23° and 24°C during July and August [6]. High relative humidity (annual mean of 83%) and high precipitation (250 mm per annum) are prevalent in the area.

3. Geological Setting and Hydrogeology

The area which is subjected to constant inundation by the water of coastal flank is geologically characterized by the Miocene Akata Formation (shales, intercalated sands, and silestone), Miocene-Pliocene Agbada Formation (sands and sandstones, intercalated with shales) and the Pliocene Benin Formation (coarse-grained sand, gravelly sands with minor intercalation of clays and shales) from top to bottom, respectively. The middle and the upper sand units of the Benin Formation constitute the major aquiferous units in the area [7, 8]. Typical boreholes in the area have 42–172 m depth, 1–55 m static water level (swl) (depth from the surface to water level in the borehole), and 39–100 m saturated thickness. Other hydrological data are 216–5304 m^2/day transmissivity, 1.2–42.5 m drawdown, and storage coefficient of 0.10–0.30 [9]. The water table varies from 1.3 m to 52 m according to [10].

4. Surface-Geophysical Method and Data Collection

Geophysical methods provide an efficient tool for characterizing subsurface geology and hydrology. The geophysical method used in this work measured the electrical resistivity using the Vertical Electrical Sounding (VES) method [11]. This was performed by using SAS 4000 ABEM Terrameter and its accessories. The apparent resistivity (ρ_a) was measured in ten locations using the following:

$$(\rho_a) = \pi \cdot \left[\frac{(\mathrm{AB}/2)^2 - (\mathrm{MN}/2)^2}{\mathrm{MN}} \right] \cdot R_a. \quad (1)$$

The equation can be simplified as in the following:

$$(\rho_a) = K \cdot R_a, \quad (2)$$

where the geometric factor $K = \pi \cdot ([(\mathrm{AB}/2)^2 - (\mathrm{MN}/2)^2/\mathrm{MN}])$, AB and MN are the current and potential electrode separations, respectively, and R_a is the resistance measured by the equipment. The potential and current electrode separations ranged between 1–40 m (MN/2 = 0.5 to 20 m) and 2–1000 m (AB/2 = 1.0 to 5000 m), respectively. Since the area has good access with avoidable obstructions, the cable spread was extended up to 1 km in order to ensure that depths above 150 m were sampled assuming that the penetration depth varies between 0.25AB and 0.5AB [12, 13]. The coordinates and elevations of the locations were taken using the Global Positioning System (GPS). The processing of apparent resistivity values with Resist Software constrained by drilled borehole lithologic information led to the determination of the model curves used in this work. From the curves, depth, thickness, and resistivity values of

different layers that the current penetrated were obtained. The measured VES in the entire area was characterized by spatial variability due to inhomogeneity of the subsurface [14–16]. The smoothening process involved averaging of the observed electrical resistivity data at crossover points or outright deleting of one of the two data sets at crossover points and other outliers that fall significantly outside the dominant trend of the curve. Any discontinuity observed after the smoothening was assumed to be geologic. The bulk water conductivity, the reciprocal of bulk resistivity, was computed from the measured resistivity.

5. Physical and Chemical Sampling and Analytical Techniques

Field sampling was carried out in the month of May 2011 and water samples were collected with a new plastic bucket and poured into 1 litre polythene bottles after measuring physical parameters such as temperature, pH, and electrical conductivity (EC) (that change rapidly with time). The EC of the unsaturated layers was estimated by saturating drilled core samples with distilled water. The parameters (pH, temperature, and water conductivity) were measured in the field using 09 Kion pH, temperature, and conductivity meter, respectively. After sampling, the bottle was capped immediately to minimize oxygen contamination and the escape of dissolved gases. The hydrochemical analysis was carried out at the Ministry of Science and Technology Central Laboratory and Aluminum Smelter Company (ASCON) Chemical Laboratory, both in Akwa Ibom State, Nigeria. The cations (Na^+, K^+, Ca^+, Mg^{2+}, Fe^{2+}, and Mn^{2+}) were determined using Atomic Absorption Spectrophotometer (UNICAM 969AAS), while the anions(Cl^- and $SO_4{}^{2-}$) were analyzed using DR 2000 Spectrophotometer at wavelength 455 nm and 450 nm. Carbonates and bicarbonates ($CO_3{}^{2-}$ and $HCO_3{}^-$) were determined titrimetrically using phenolphthalein and methyl orange indicator method [17]. Water samples meant for anion determination were acidified and the choice of acid depended on the anion. For example, water sample meant for ions determination was primed with 0.5 M solution of nitric acid to keep the ions in solution.

6. Data Analysis, Interpretation, and Discussion of Results

6.1. Geophysical Data Analysis and Results. Smoothing of field data by manual plotting on a bilogarithmic graph for curve matching and computer modelling of the result from manual plotting were employed in the reduction of field data [18–20] to their equivalent geological models. Transformation of the measured apparent resistance R_a to their corresponding apparent resistivity ρ_a was achieved using (1). The manual procedure involves plotting the computed apparent resistivity data on a bilogarithmic graph and, where necessary, the curves generated were smoothened to remove the effects of lateral inhomogeneities and other forms of noisy signatures in the smoothened curve were attributed to vertical variation of electrical resistivity with depth. The smoothened curves were quantitatively interpreted in terms of true resistivity and thickness by a conventional manual curve matching procedure using master curves and auxiliary chart [18, 21]. The conventional curves and auxiliary charts (theoretical curves) used in the interpretation aided in obtaining a good fit between the observed field curves and the theoretical curves during total and partial matching. Software programs were later used to improve upon the manually interpreted results. Since the data were acquired at different times, several VES modelling Software programs including Resist [22], Ato [23], and Res1D [24] were used in modelling the data and the results were later transformed to their equivalent geological models. The primary layer parameters comprising resistivity, thicknesses, and depths obtained from the manual interpretation stage were keyed as inputs into some of the computer modelling Software programs (Resist and Res1D only). The computer Software used these parameters to generate data for the estimated model and compared the computed data with their measured counterpart. The extent of fit between the calculated and the measured data sets was assessed using the root mean square error (RMS) technique in which 10% was set as the maximum accepted value. Representative examples of modelled VES curves obtained within the dumpsite and its environs after the smoothing and modelling exercises are shown in Figures 2, 3, and 4 for the three transects considered. For VES far from the dumpsite, a good correlation was observed between the electrical resistivity derived 1D subsurface model and the geology model, while some disconformities were noticed in VES closed to the dumpsite as shown in Figures 2, 3, and 4. The observed variations are attributable to the leachate emanated from the garbage in the dumpsite. Table 1 shows the inferred bulk resistivity values and their layers as well as the corresponding water resistivities. Table 1 also shows the bulk and fluid conductivities of the penetrated layers and the borehole depths in the study area.

Resistivity cross sections were constructed for each of the transects with the aid of Surfer Golden Software Inc., USA, by combining the inverted results of the Schlumberger soundings as shown in Figures 5, 6, and 7. To construct the resistivity cross sections, the inverted electrical resistivities were sampled with depths. The vertical variation in electrical resistivity with depth was gridded using the kriging gridding technique available in the Surfer package [25]. The interpolated electrical resistivities were imaged along the profile.

7. Interpretation and Discussion of VES Results

The VES results from the study area are generally characterised with high and low conductivities at various depths and locations (see Figures 2, 3, and 4). This is conveyed in the geoelectric cross sections that strategically show zones that have high resistivity (low conductivity) and zones that have low resistivity (high conductivity) (see Figures 5, 6, and 7). The conductive zones have geologic formations that

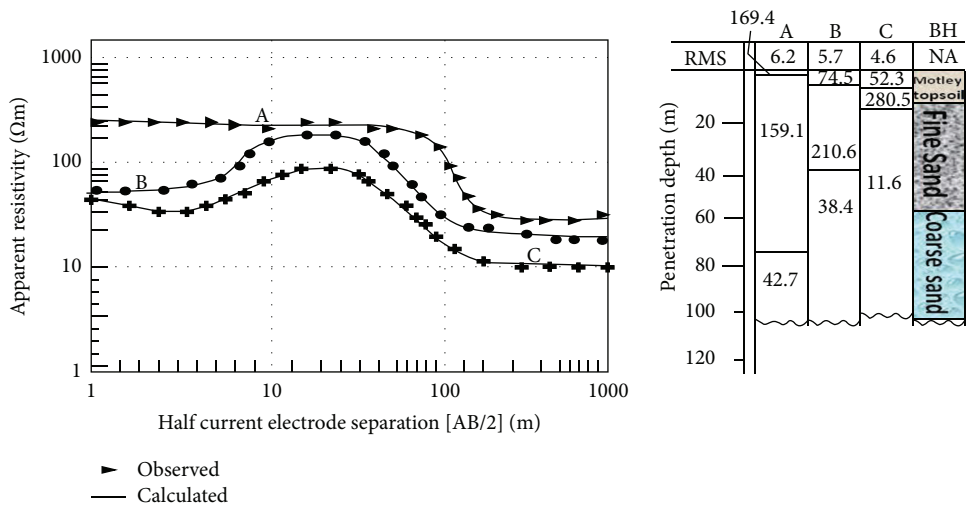

Figure 2: Typical VES curves and modelled results obtained along A-A[1] profile (A Agric. secretariat, B IK. club, and C Local G. Area secretariat).

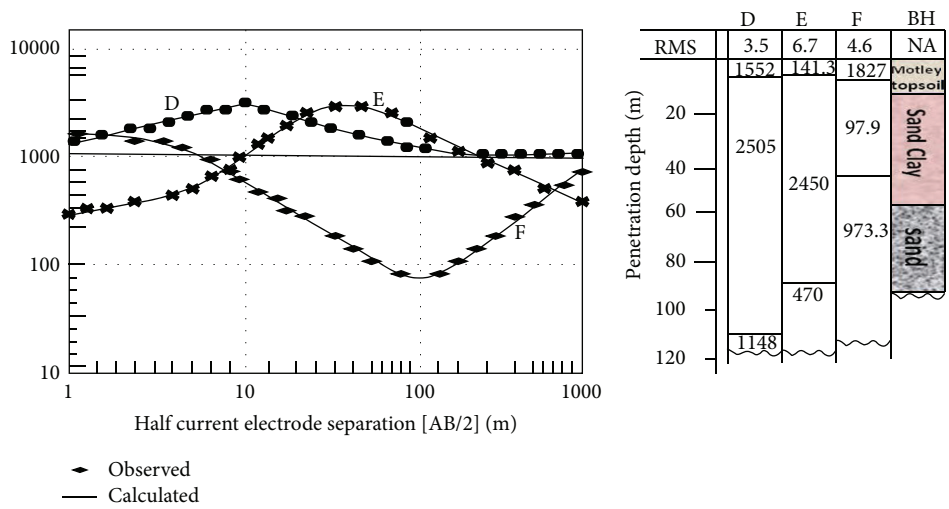

Figure 3: Typical VES curves and modelled results obtained along B-B[1] profile (D FRS Office, E Ik. Club and F FCMB).

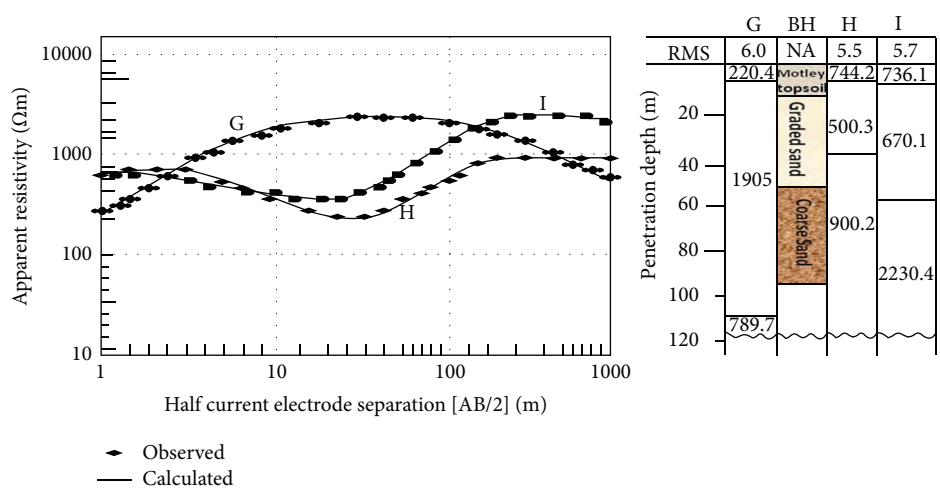

Figure 4: Typical VES curves and modelled results obtained along C-C[1] profile (G Akwa Savings & Loans H Fire service station and I Theological College).

Table 1: Summary of measured geoelectric parameters and depths of boreholes used as constraints in the study area.

Location	Bulk resistivity (Ωm)			Water resistivity (Ωm)			Bulk conductivity ($\Omega^{-1}m^{-1}$)			Water conductivity ($\Omega^{-1}m^{-1}$)			depth (m)		Borehole depth (m)
	ρ_{b1}	ρ_{b2}	ρ_{b3}	ρ_{1w}	ρ_{2w}	ρ_{3w}	σ_{b1}	σ_{b2}	σ_{b3}	σ_{1w}	σ_{2w}	σ_{3w}	d_1	d_2	
Agric. secretariat [A]	169.4	159.1	17.7	14.8	14.1	5.9	0.0059	0.0063	0.1695	0.067	0.071	0.0709	0.8	76.7	78.0
IK. Club [B]	74.5	210.6	38.4	10.9	13.3	9.9	0.0134	0.0047	0.10101	0.092	0.075	0.0752	2.4	39.1	85.0
Local. G. Area secretariat [C]	52.3	280.5	11.6	15.1	11.5	6.7	0.0191	0.0036	0.14925	0.066	0.087	0.0867	4.1	11.4	58.6
Queen street	68.5	260.1	836.9	11.9	11.9	26.0	0.0146	0.0038	0.03846	0.084	0.084	0.0840	3.9	14.9	—
FRS office [D]	1551.9	2504.6	1148.2	39.9	29.9	12.6	0.0006	0.0004	0.00090	0.025	0.033	0.0334	3.3	110.5	95.0
FCMB [F]	1826.8	97.9	973.9	43.9	35.6	28.2	0.0005	0.0102	0.07752	0.023	0.028	0.0280	3.6	40.1	68.9
Theological college [I]	736.1	670.7	2230.4	14.9	18.4	12.9	0.0014	0.0015	0.00045	0.065	0.054	0.0543	4.6	59.4	54.0
IK. hospital [E]	141.3	2450.3	470.0	12.9	16.6	19.4	0.0071	0.0004	0.04367	0.078	0.060	0.0602	2.0	91.8	75.0
Akwa savings and loans [G]	220.4	1905.2	789.7	11.6	22.9	22.9	0.0045	0.0005	0.04367	0.086	0.043	0.0437	4.9	117.5	80.0
Fire service station [H]	744.1	500.3	900.2	14.9	23.7	26.8	0.0013	0.0020	0.0011	0.067	0.042	0.0709	5.3	38.1	52.5

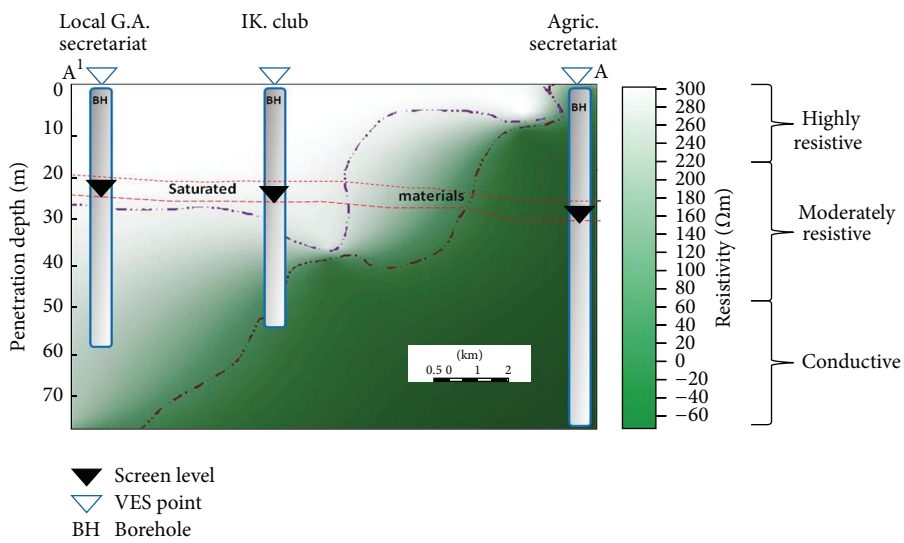

Figure 5: Resistivity cross section along a profile from Agric. secretariat to Local G. Area Secretariat (A-A^1).

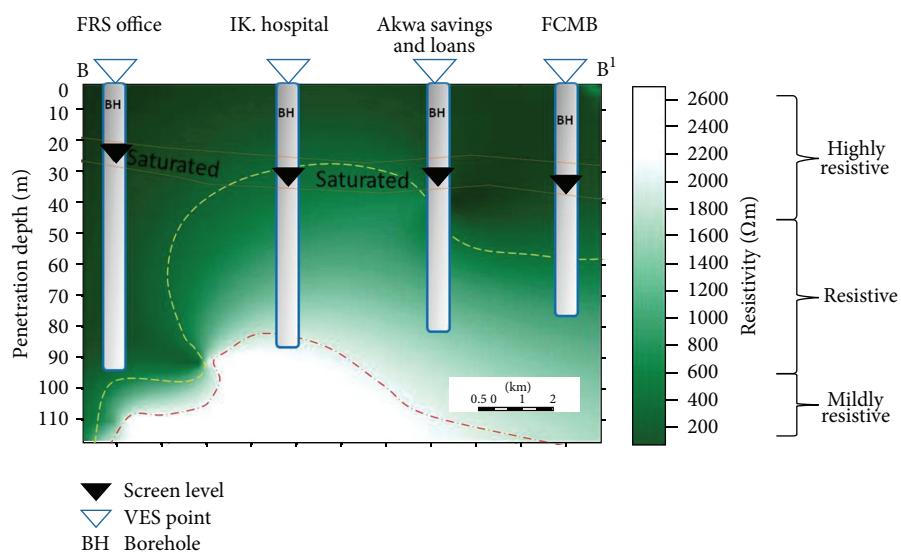

Figure 6: Resistivity cross section along a profile from FRS Office to FCMB (B-B^1).

are associated with leachate contaminations. Figure 5 (A-A^1 profile) shows on the average transitions of resistivity variations from resistive zone to conductive zone. The resistivity increases diagonally downward from Agric. Secretariat (closed to dumpsite) to the Local G. Area Secretariat (away from dumpsite). Similarly, conductivity increases diagonally from the deeper layer of VES at the Local G. Area Secretariat to the surficial layer at the Agric. Secretariat. The observation in this profile explains the effect of massive percolation of tissue fluid (leachate) into the subsurface within the dumpsite environment. The borehole water at Agric. Secretariat appears to be influenced by fluid emanated from garbage dumped in the dumpsite. The distribution of the bulk and fluid conductivities as shown in the Table 1 changes from place to place and within the depths penetrated in the profile. In Figure 6 (profile B-B^1) of resistivity cross section, the resistivity increases with depth at the various VES points except at FCMB where resistivity inversion is noticed at the second layer of the transition. Combining all the VES, the resistivity cross section traversing B-B^1 profile shows higher resistivity which implies low conductivity at higher depths. In Figure 7, the resistivity cross section traversing C-C^1 profile shows, in average, higher values within the southwest-northeast diagonal trend. In this resistivity image cross section, three transitions are generally noticed. These are highly resistive, moderately resistive, and mildly conductive zones. Generally, for A-A^1 profile which is nearer to the dumpsite the sampled depths appear to be conductive (less resistive) ranging from the topmost layer of Agric. secretariat-nearest to the dumpsite, to the deepest layer of Local G. Secretariat farther away from the dumpsite. This implies that the conductive tissue fluid from the dumpsite leaches

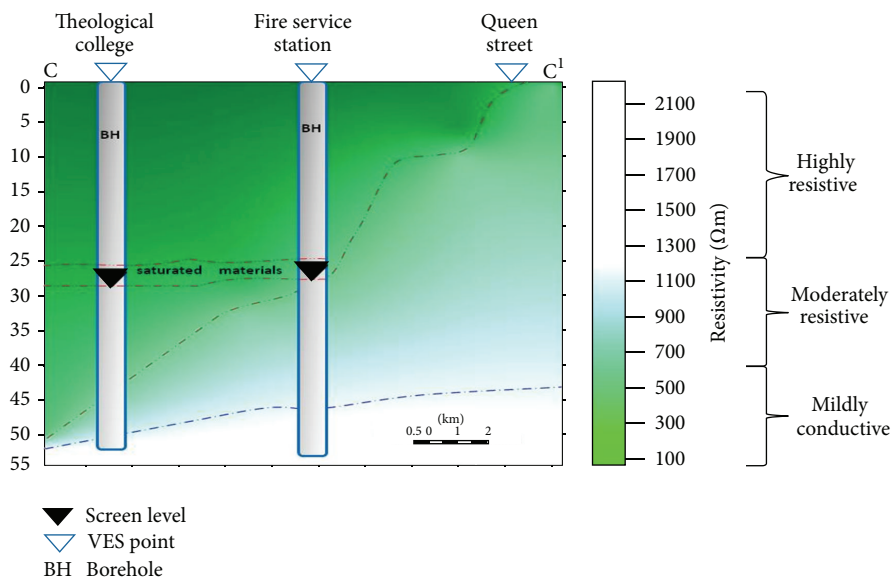

Figure 7: Resistivity cross section along a profile from Agric. secretariat to Local G. Area Secretariat (C-C^1).

the subsurface within its axis diagonally, from top to bottom. This is the reason for the observed trend in the resistivity image cross section of A-A^1 profile. For B-B^1 and C-C^1 profiles which are about 1 km away from the dumpsite, resistivity inversion occurs as resistivity on the average increases with depth due to the assumed normal compaction or lithification of sediments at deeper depth of burial.

8. Interpretation of Water Resistivity and Bulk Resistivity Interactions

Water and bulk resistivities determined in Table 1 were plotted as shown in the crossplots of Figures 8, 9, and 10 for first, second, and third layers, respectively. The plots generated site dependent generalised model given in the following:

$$y = Ae^{bx}, \tag{3}$$

where y and x represent the water resistivity and bulk resistivity, respectively. A and b in (3) are site dependent constants. The water resistivity y increases exponentially with bulk resistivity x. Specifically, A is the threshold or ambient water resistivity, which depends on the artificially induced conductivity of pore fluid of the layer considered. The parameter b is the fluid-soil matrix mixing dimensionless constant which depends on the bulk conductivity and the overall formation factor, the ratio of bulk resistivity to water resistivity of the medium. From the first layer, the equation generated in Figure 8 has the values $A = 11.183\,\Omega$m and $b = 0.0007$. These values, respectively, signify the inferred ambient water resistivity and fluid-soil matrix mixing constant for layer one. Similarly, for the second and third layers, A and b are, respectively, 11.3290 Ωm and 0.0005 and 7.6938 Ωm and 0.0007. The observed values on the average show that layers one and two are similar in terms of the ambient water resistivities and fluid-soil matrix mixing constants. However, while b for the third layer conforms to the first two layers, A deviates significantly. Although the degree of mixing is approximately the same due to similarity in geologic formations, there is alteration in the threshold artificially induced water conductivity, on the average, from 0.0888 to 0.1300 Siemens between layer one and layer three. From this range, the artificially induced fluid that influences the natural conductivity is more significant on the deeper layers than the surficial layers. This could be attributable to the continuous accumulation of leachate that drains or leaches downwards from the topmost layer to the deeper layer. The observed unconformity of the resistivity image cross section to the borehole information obtained when the borehole was drilled is an indication of the effect of leachate on the sandy formations and within the layers of the subsurface. Since the aquifer protecting layer's longitudinal conductance S (the ratio of top layer thickness to top layer resistivity) is generally less than $1\,\Omega^{-1}$ (i.e., $S \ll 1\,\Omega^{-1}$), as observed from Table 1 for all the VES locations, the aquifers are poorly protected generally. The underlying layers also have S values that are less than 1 and this paves the way for the conductive contaminated fluid from the dumpsite to drain into the subsurface thereby affecting the threshold natural resistivity or conductivity in the deeper layers.

9. Interpretation of Physicochemical Properties of the Groundwater Samples Measured from the Study Area

The parameters measured in the study area include pH, EC (μS/cm), and temperature (°C), for physical parameters and Na^+, K^+, Ca^{2+}, Mg^{2+}, Fe^{2+}, Cl^-, $SO_4{}^{2-}$, $HCO_3{}^-$, $PO_4{}^{3-}$, $NO_3{}^-$, F^-, As, Mn, and Cu^{2+} all measured in (Mg/L) for hydrochemical parameters (see Table 2). The mean value for each of the parameters detectable was calculated except for ions

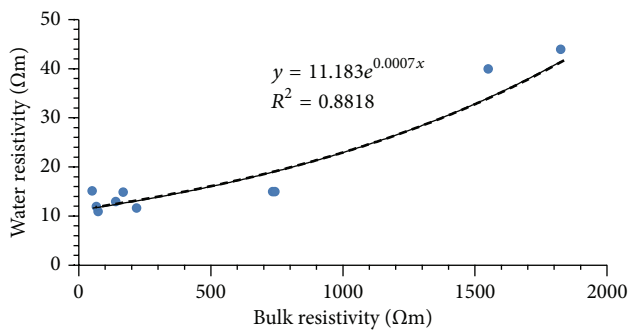

Figure 8: A graph of first layer water resistivity against bulk resistivity.

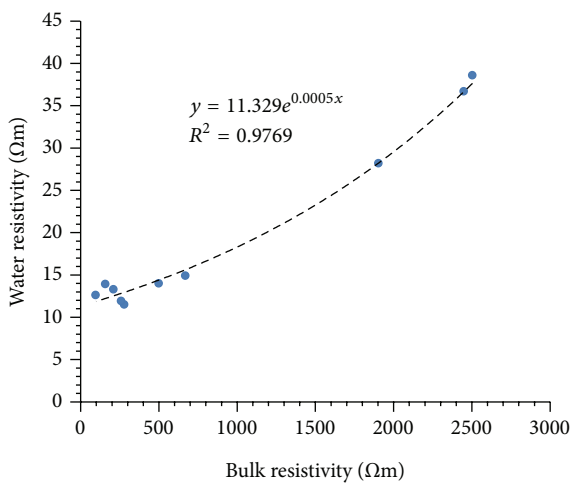

Figure 9: A graph of second layer water resistivity against bulk resistivity.

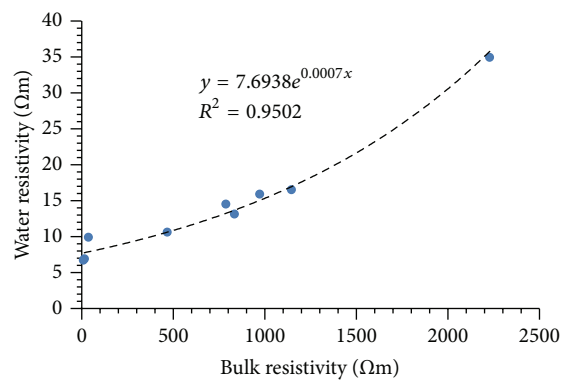

Figure 10: A graph of third layer water resistivity against bulk resistivity.

that were below detectable limit (BDL). The mean values for ions were compared with the WHO standard values available. The available WHO standard conforms to some ions except $K^+ > 2.0$, $Mg^{2+} > 1.0$, $F^- > 0.01$, Mn > 0.01, and $Cu^{2+} > 0.01$ Mg/L which are beyond the acceptable WHO standard for drinking water. The high values of the above ions within the dumpsite and its vicinity in Table 2, could be due to the hydrolysis and the resulting leaching from the contaminated sources. Hydrolysis and consequent leaching leads to the precipitation of the above ion species in water sample used. Correlation in Table 3 shows that though most of the ions are higher than the WHO standard, correlation indices between the anion and cation are significantly low. This implies that the concentration of the paired ions in Table 3 is insignificant in the water sample. In all the water samples chemically analysed, carbonate (CO_3^{2-}) was below detection level (BDL). This further confirms that the dumpsite and its environs are devoid of normal carbonate-rich compounds. However, the availability of bicarbonate (HCO_3^-) up to 172 Mg/L suggests the dissolution of carbonates and reaction of silicates with carbonic acid which results in high concentration of HCO_3^- in the water samples obtained from the study. Although the concentration of Ca^{2+} is low, the high value of Mg^{2+} suggests that the water samples within the dumpsite and its vicinity may be temporarily hard due to the possibility of formation of $Mg(HCO_3)_{2(aq)}$.

In terms of the physical parameters, temperature, pH, and electrical conductivity (EC) were measured for the water samples collected within and around the dumpsite. The measured temperature values ranged from 27.8 to 29.8°C and the mean value was 28.9°C. The temperature values were found to remain approximately constant throughout the duration of the field work. This is an advantage that groundwater has over surface water. The pH values ranged from 6.5 to 8.5 and the mean value was 7.5. The mean pH value result suggests that the water quality is close to neutrality level with values varying from 6.7 to 8.5. These values fall within WHO acceptable standard range of 6.5–8.5 [26]. The slightly acidic nature of the water can be attributed to the dissolution and draining of decomposed vegetative materials and other biodegradable wastes from dumping refuse and its surroundings by runoff that are in hydraulic connection with the local groundwater system [27, 28]. The water conductivity ranged from 34 to 1183 μS/cm. The average value was 229 μ/cm. The relatively high values obtained at some locations are symptomatic of the abundance of free ions in the water which could be attributed to the existence of equilibrium between the water and the soluble leachate-loaded contamination plume that dissolves into the soil [29]. The conductivity values are below the WHO standard value of 1,400 μS/cm [30]. Despite the known dependence of EC on the mobility of free ions in the water, the EC of the water also depends on the amount of dissolved substances in the water. Several researchers including [31, 32] have discussed the influence of EC on water quality. Ordinarily, the EC will be low for good quality water with low total dissolved solids (TDS). Thus, high aquifer resistivities can be delineated with areas with low TDS. The relatively high concentration of K^+, Mg^{2+}, F^-, Mn, and Cu^{2+} in the repository of groundwater can also be due to tectonically induced secondary structures like, divide, fault lineament, and fold within the sedimentary facies which jointly creates rooms for the leaching, precipitation, and their dissolution in the subsurface water [33]. These

Table 2: Summary of measured hydrochemical and some physical parameters for water sample used.

S/N	Location	Temp. T (°C)	pH	Cond. (μS/cm)	Na^+ (Mg/L)	K^+ (Mg/L)	Ca^+ (Mg/L)	Mg^+ (Mg/L)	Fe^+ (Mg/L)	SO_4^{2-} (Mg/L)	Cl^- (Mg/L)	PO_4^{3-} (Mg/L)	CO_3^{2-} (Mg/L)	HCO_3^- (Mg/L)	NO_3^- (Mg/L)	F^- (Mg/L)	Mn (Mg/L)	As (Mg/L)	Cu (Mg/L)
BH1	IK. hospital	29.7	6.9	67	6.9	2.1	11.6	1.8	0.04	1.0	22.9	0.8	BDL	245	3.9	0.3	0.003	0.01	0.10
BH2	FRS office	28.6	7.6	88	7.8	4.0	3.0	2.0	0.11	6.0	17.9	1.2	BDL	156	1.9	0.7	0.004	0.01	1.20
BH3	IK. club	29.2	8.1	1183	11.9	18.5	15.9	3.5	0.03	1.0	76.9	2.1	BDL	209	41.0	0.4	0.001	0.01	0.08
BH4	Local. G. Area secretariat	28.8	8.2	96	7.9	0.6	9.9	0.8	0.05	1.2	47.0	2.0	BDL	80	1.7	0.3	0.006	0.01	0.01
BH5	Akwa savings and Loans	29.0	7.5	34	4.9	1.9	7.2	0.4	0.07	3.0	58.9	1.3	BDL	215	1.8	0.6	0.003	0.01	0.01
BH6	FCMB	27.9	6.5	65	5.0	3.0	5.4	5.6	0.01	2.0	43.7	1.3	BDL	240	1.3	0.3	0.002	0.01	0.01
BH7	Theological college	29.8	6.7	77	6.5	1.7	3.9	2.3	0.09	3.2	30.9	0.9	BDL	221	4.6	0.5	0.007	0.01	0.08
BH8	Fire service station	28.9	7.8	129	8.1	2.5	9.0	3.5	0.06	2.0	55.6	1.5	BDL	171	34.0	0.3	1.001	0.01	0.06
BH9	Queen street	27.9	7.4	45	4.3	3.7	0.9	5.1	0.03	7.0	34.9	1.1	BDL	100	1.6	0.4	0.008	0.01	0.03
BH10	Agric secretariat	29.5	8.5	509	8.9	0.9	1.5	5.9	0.06	3.6	66.8	2.2	BDL	80	42.0	0.5	1.001	0.01	0.05
	Minimum	27.9	6.7	34	4.9	0.6	0.9	0.4	0.01	1.0	17.9	0.8	BDL	80	1.3	0.3	0.001	0.01	0.01
	Maximum	29.8	8.2	1183	11.9	18.5	15.9	5.9	0.11	7.0	76.9	2.2	BDL	240	42.0	0.7	1.002	0.01	1.20
	Range	27.9–29.8	6.7–8.5	34–1183	4.9–11.9	0.6–18.5	0.9–15.3	0.4–5.9	0.01–0.11	1.0–7.0	17.9–76.9	0.8–2.2	BDL	80–240	1.3–42.0	0.3–0.7	0.001–1.002	0.01–0.01	0.01–1.20
	Mean	28.9	7.5	229	7.2	3.9	6.8	3.1	0.06	3.0	45.6	1.4	BDL	172	13.4	0.4	0.204	0.01	0.16
	WHO standard 2006/2010	NS	6.5–8.5	1400	200	2.0	250	1.0	1.0	40.0	200	NS	NS	NS	44.0	0.01	0.01	0.01	0.01

Table 3: Calculated ion pair correlation indices.

Ion pair	Inferred correlation index for ion pair
Na^+-SO_4^{2-}	0.17
Na^+-Cl^-	0.26
Mg^{2+}-SO_4^{2-}	0.06
Ca^{2+}-Cl^-	0.14
K^+-SO_4^{2-}	0.04
SO_4^{2-}-Cu^{2+}	0.24
SO_4^{2-}-As	0.00
NO^{3-}-As	0.00

secondary structures also create room for the multiple aquifer units in the study area.

10. Conclusions

In the course of using integrated approach to investigate the effect of leachate on ground water repository of Ikot Ekpene dumpsite in Akwa Ibom State, Nigeria, the study area, information generated from vertical electrical sounding, geological and hydrogeochemical techniques have been integrated and used in mapping shallow subsurface electrostratigraphy. The results aided in identifying the aquiferous horizons and their geometry and assessing the effects of leachate on the groundwater within the axis of Ikot Ekpene dumpsite. From the primary geoelectrical parameters inferred, aquifers are generally open or unconfined in the area. They are anisotropic and localized in both lateral and vertical extents. The electrical resistivity values of the aquiferous horizon were observed to be lower (<300 Ωm) in the VES data close to the dumpsite (profile A-A^1) and relatively higher than those VES away from the dumpsite (profiles B-B^1 and C-C^1) in the study area. Thus, the distribution of water conductivity in the area as shown in Table 1 follows the resistivity pattern. The interpretation of resistivity data and its inferred section in profile A-A^1 shows that the conductive fluid from the dumpsite has dominant effect on the subsurface for VES data closer to the dumpsite than those VES data relatively farther away from it. The effect is eminent as it is shown in the diagonal pattern of flow from top to bottom. For profiles B-B^1 and C-C^1 which are farther away from the dumpsite, the resistivity seems on the average to be increased downward as it is expected in a normal situation where variations in resistivity with depth of burial are only due to lithologic differentiation caused by age and cementation or compaction. From the resistivity data analysis and the pore water measurement, water resistivity increases exponentially with bulk resistivity in the different layers of the subsurface sampled. The threshold or ambient water resistivity depends on the artificially induced conductivity of pore fluid for the layers considered. The high range of water conductivity (34–1183 μS/cm) in the borehole is attributable to the unequal draining of the subsurface by the conductive leachate-loaded plume which decreases with increasing distance from the dumpsite location. The parameters realised from the model generated from bulk and water resistivity can be used to explain the extent of dissolution of leachate in water repositories within and away from the dumpsite.

Hydrochemical results show that repository of groundwater contains little or no CO_3^{2-}. However, the subsurface is enriched with HCO_3^- due to the reaction of silicates with carbonic acid which results in the high concentration of HCO_3^- in groundwater in all the geologic formations. Although some ions were below the available WHO standards, some were above the acceptable standard. The high values of some hydrochemical species can be attributed to the dissolution and precipitation of the leachate-loaded contamination plume within the subsoil. This and other tectonically induced secondary structures like divide, fault lineament, and fold within the sedimentary facies cause wide variations in resistivities and conductivities within the subsurface of the study area. In effect, this influences the resistivity and conductivity of groundwater in the study area. The chemical, physical, and geostatistical parameters generated in this work can be used in monitoring the water quality within the vicinity of the dumpsite from time to time.

Conflict of Interests

The authors declare that there is no conflict of interests regarding the publication of this paper.

References

[1] E. Atekwana, E. Atekwana, and R. Rowe, "Relationship between total dissolved solids and bulk conductivity at a hydrocarbon-contaminated aquifer," in *Proceedings of the Symposium on the Application of Geophysics to Engineering and Environmental Problems*, pp. 228–223, 2003.

[2] A. Edet and R. H. Worden, "Monitoring of the physical parameters and evaluation of the chemical composition of river and groundwater in Calabar (Southeastern Nigeria)," *Environmental Monitoring and Assessment*, vol. 157, no. 1–4, pp. 243–258, 2009.

[3] A. Papaioannou, P. Plageras, E. Dovriki et al., "Groundwater quality and location of productive activities in the region of Thessaly (Greece)," *Desalination*, vol. 213, no. 1–3, pp. 209–217, 2007.

[4] K. A. Yusuf, "Evaluation of groundwater quality characteristics in Lagos-City," *Journal of Applied Sciences*, vol. 7, no. 13, pp. 1780–1784, 2007.

[5] P. Soupios, I. Papadopoulos, M. Kouli, I. Georgaki, F. Vallianatos, and E. Kokkinou, "Investigation of waste disposal areas using electrical methods: a case study from Chania, Crete, Greece," *Environmental Geology*, vol. 51, no. 7, pp. 1249–1261, 2007.

[6] N. J. George, A. E. Akpan, and I. B. Obot, "Resistivity study of shallow aquifers in the parts of Southern Ukanafun Local Government Area, Akwa Ibom State, Nigeria," *E-Journal of Chemistry*, vol. 7, no. 3, pp. 693–700, 2010.

[7] O. E. Esu and A. E. Amah, "Physico-chemical and Bacteriological quqlity of natural water in parts of Akwa Ibom and Cross River States, Nigeria," *Global Journal of Pure and Applied Sciences*, vol. 5, no. 4, pp. 525–531, 1999.

[8] A. E. Akpan, A. N. Ugbaja, and N. J. George, "Integrated geophysical, geochemical and hydrogeological investigation of shallow groundwater resources in parts of the Ikom- Mamfe Embayment and the adjoining areas in Cross River State, Nigeria," *Environmental Earth Sciences*, vol. 70, no. 3, pp. 1435–1456, 2013.

[9] O. E. Esu, C. S. Okereke, and A. E. Edet, "A regional hydrostratigraphic study of Akwa Ibom State, South-eastern Nigeria," *Global Journal of Pure and Applied Sciences*, vol. 5, no. 9, pp. 89–96, 1999.

[10] K. K. Roy and H. M. Elliot, "Some observations regarding depth of exploration in D.C. electrical methods," *Geoexploration*, vol. 19, no. 1, pp. 1–13, 1981.

[11] K. P. Singh, "Nonlinear estimation of aquifer parameters from surficial resistivity measurements," *Hydrology and Earth System Sciences*, vol. 2, pp. 917–938, 2005.

[12] R. D. Ogilvy, P. I. Meldrum, O. Kuras et al., "Automated monitoring of coastal aquifers with electrical resistivity tomography," *Near Surface Geophysics*, vol. 7, no. 5-6, pp. 367–375, 2009.

[13] C. M. A. Ademoroti, *Standard Methods for Water and Effluent Analysis*, 1st edition, 1996.

[14] V. Chakravarthi, G. B. K. Shankar, D. Muralidharan, T. Harinarayana, and N. Sundararajan, "An integrated geophysical approach for imaging subbasalt sedimentary basins: case study of Jam River Basin, India," *Geophysics*, vol. 72, no. 6, pp. B141–B147, 2007.

[15] A. A. R. Zohdy, "The auxiliary point method of electrical sounding interpretation and its relationship to the Dar-Zarouk parameters," *Geophysics*, vol. 30, pp. 644–660, 1965.

[16] A. A. R. Zohdy, G. P. Eaton, and D. R. Mabey, *Application of Surface Geophysics to GroundWater Investigation. USGS Techniques of Water Resources Investigations*, Book 2, chapter D1, 1974.

[17] A. I. Tsafe, L. G. Hassan, D. M. Sahabi, Y. Alhassan, and B. M. Bala, "Assessment of heavy metals and mineral compositionsin some solid minerals deposit and water from a gold mining area of Northern Nigeria," *International Research Journal of Geology and Mining*, vol. 2, no. 9, pp. 254–260, 2012.

[18] E. Orellana and A. M. Moony, "Master curve and tables for vertical electrical sounding over layered structures. Interciencia, Escuela Papadopoulou MP, Varouchakis EA, Karatzas GP, (2010) Terrain discontinuity effects in the regional flow of a Complex Karstified Aquifer," *Environmental Modeling and Assessment*, vol. 15, no. 5, pp. 319–328, 1966.

[19] V. Vender BPA, "A computer processing package for D.C. Resistivity interpretation for an IBM compatibles," *ITC Journal*, vol. 4, 1988.

[20] A. A. R. Zohdy, "A new method for the automatic interpretation of Schlumberger and Wenner sounding curves," *Geophysics*, vol. 54, no. 2, pp. 245–253, 1989.

[21] M. H. Loke, RES1D version 1. 0 for Windows 95/98/Me/2000/NT. 1-D Resistivity, IP & SIP Inversion and forward modelling for Wenner and Schlumberger arrays, 2001.

[22] K. S. Gemail, A. M. El-Shishtawy, M. El-Alfy, M. F. Ghoneim, and M. H. Abd El-Bary, "Assessment of aquifer vulnerability to industrial waste water using resistivity measurements. A case study, along El-Gharbyia main drain, Nile Delta, Egypt," *Journal of Applied Geophysics*, vol. 75, no. 1, pp. 140–150, 2011.

[23] WHO, *Guidelines for Drinking Water Quality*, vol. 1 of *Recommendations*, WHO, Geneva, Switzerland, 2nd edition, 2004.

[24] M. Ketata, M. Gueddari, and R. Bouhlila, "Suitability assessment of shallow and deep groundwaters for drinking and irrigation use in the El Khairat aquifer (Enfidha, Tunisian Sahel)," *Environmental Earth Sciences*, vol. 65, no. 1, pp. 313–330, 2012.

[25] N. J. George, A. O. Akpan, and A. A. Umoh, "Preliminary geophysical investigation to delineate the groundwater conductive zones in the coastal region of Akwa Ibom State, Southern Nigeria, around the Gulf of Guinea," *International Journal of Geosciences*, vol. 4, pp. 108–115, 2013.

[26] J. D. Hem, "Study and interpretation of the chemical characteristics of natural water," *US Geological Survey Water-Supply Paper*, vol. 2254, 1985.

[27] WHO, *Drinking Water Standards, Monitoring and Reporting*, vol. 1 of *Recommendations*, WHO, Geneva, Switzerland, 2nd edition, 2010.

[28] R. K. Frohlich and D. W. Urish, "The use of geoelectrics and test wells for the assessment of groundwater quality of a coastal industrial site," *Journal of Applied Geophysics*, vol. 50, no. 3, pp. 261–278, 2002.

[29] R. Barker, T. V. Rao, and M. Thangarajan, "Delineation of contaminant zone through electrical imaging technique," *Current Science*, vol. 81, no. 3, pp. 277–283, 2001.

[30] M. N. Tijani, "Evolution of saline waters and brines in the Benue-Trough, Nigeria," *Applied Geochemistry*, vol. 19, no. 9, pp. 1355–1365, 2004.

[31] N. J. Raju, P. Ram, and S. Dey, "Groundwater quality in the lower Varuna River basin, Varanasi district, Uttar Pradesh," *Journal of the Geological Society of India*, vol. 73, no. 2, pp. 178–192, 2009.

[32] R. Barker, T. V. Rao, and M. Thangarajan, "Delineation of contaminant zone through electrical imaging technique," *Current Science*, vol. 81, no. 3, pp. 277–283, 2001.

[33] A. A. Elueze, J. O. Omidiran, and M. E. Nton, "Hydrogeochemical investigation of surface water and groundwater around Ibokun, Ilesha area, Southwestern Nigeria," *Journal of Mining and Geology*, vol. 40, no. 1, pp. 57–64, 2004.